Exfoliation and Chemical Modification Using Microwave Irradiation Affording Highly Functionalized Graphene

Solon P. Economopoulos,[†] Georgios Rotas,[†] Yasumitsu Miyata,[‡] Hisanori Shinohara,[‡] and Nikos Tagmatarchis[†,*]

[†]Theoretical and Physical Chemistry Institute, National Hellenic Research, Foundation, 48 Vassileos Constantinou Avenue, 11635 Athens, Greece, and [‡]Department of Chemistry, Nagoya University, Nagoya 464−8602, Japan

ABSTRACT Efficient exfoliation of graphite flakes by sonicating them in benzylamine was accomplished, affording stable suspensions of few-layers graphene. The latter were chemically modified following the Bingel reaction conditions, with the aid of microwave irradiation, producing highly functionalized graphene-based hybrid materials. The resulting hybrid materials, possessing cyclopropanated malonate units covalently grafted onto the graphene skeleton, formed stable suspensions for several days in a variety of organic solvents and were characterized by diverse and complementary spectroscopic, thermal, gravimetric, and high-resolution electron microscopy techniques. When a malonate derivative, bearing the electro-active extended tetrathiafulvalene (exTTF) moiety, was synthesized and used for the functionalization of graphene, energy dispersive X-ray (EDX) analysis verified the presence of sulfur in the corresponding graphene-based hybrid material. Moreover, the redox potentials of the exTTF-graphene hybrid material were determined by electrochemistry, while the formation of a radical ion pair that includes one-electron oxidation of exTTF and one-electron reduction of graphene was suggested with the energy gap of $(graphene)^{\bullet-}$—$(exTTF)^{\bullet+}$ being calculated as 1.23 eV.

KEYWORDS: graphene · exfoliation · functionalization · microwaves · characterization

Ever since its introduction by Novoselov and co-workers in 2004,[1] researchers turned their attention on the novel and seemingly abundant graphene material. Produced from graphite, graphene sheets can be isolated without costly and elaborate techniques, offer an array of desirable properties, and enrich the family of carbon allotropes along with single walled carbon nanotubes (SWCNTs),[2] fullerenes,[3] and single walled carbon nanohorns (SWCNHs).[4] Graphene sheets open new pathways toward realization of nanotechnology applications[5,6] and may even be the long-awaited replacement of silicon in electronic devices.[7]

Offering electrical conductivity,[8−13] spin transport,[14] and ferromagnetism,[15] as well as good mechanical[16−20] and excellent thermal properties,[21] graphene at the same time is free of some of the drawbacks that hamper SWCNTs such as metal impurities.[22] Its 2D geometry, comprising a single layer of graphite, allows for some interesting applications, like conducting films[23] where its carbon nanostructured counterparts such as fullerenes (0D), SWCNTs (1D), and SWCNHs (3D) fall short. Altering the 2D carbon lattice of graphene by covalently introducing functional moieties (*i.e.,* photo- and/or electroactive species) is a key-step toward the preparation and development of some novel graphene-based nanohybrids potentially suitable in optoelectronics.[24] However, like its parent graphite material, graphene sheets remain insoluble in all solvents and additional steps must be taken to overcome this disadvantage.

Another obstacle stems from the process to obtain graphene sheets from graphite in high yields. Many studies emerged over the last years to address this issue. To this end, several methodologies exist, including chemical vapor deposition,[25] epitaxial growth,[26,27] carbon nanotube cutting,[28,29] mechanical exfoliation,[30,31] chemical reduction,[16,32,33] and direct sonication.[34,35] Each of these methods presents both advantages and disadvantages, dealing with cost and scalability. Once in graphene form, the material can undergo further chemical modification to decorate it with functional groups that can add to the properties of the material, for example, enhanced solubility, *etc.*

Of the aforementioned approaches toward obtaining graphene sheets, the direct sonication method seems to be the most attractive due to its simplicity. Coleman and co-workers suggested[34] that in order to "solubilize" graphene, the solvent used should provide strong interactions with the layers, rivaling the van der Waals interlayer forces present in graphene multilayers/graphite. Direct sonication, also seems to be the only

*Address correspondence to tagmatar@eie.gr.

Received for review July 22, 2010 and accepted November 09, 2010.

Published online November 16, 2010.
10.1021/nn101735e

alternative to chemical reduction, for the scalable production of graphene.

Chemical reduction of graphene involves, initially, direct oxidation of graphite[36] introducing numerous defects and oxygenated species. The resulting material is graphene oxide (GO) and is soluble in aqueous media. The presence of defect sites naturally disrupts the π-planarity of the material making GO an insulator.[37,38] To remedy this fundamental shortcoming, GO can undergo thermal or chemical reduction[39] for the removal of the oxygen sites which are faced with the task of completely removing all the introduced defects and returning the carbon material to its conducting state. However, this chemically converted graphene[40] naturally has the tendency to form aggregates limiting its applications and most commonly requiring stabilization in a substrate prior to or after removal of the oxygen defects.[41,42] On the other hand, direct sonication of graphite using an appropriate solvent is favorable due to its low introduction of defect sites, which are mostly edge-situated, rather than planary, leaving intact the electrical properties of the material.[43]

Covalent functionalization of graphene has been on the forefront of researchers' interest either as a way to stabilize and obtain graphene from graphite, or as a means to enrich graphene's properties.[24] The Bingel cyclopropanation reaction is commonly applied for the functionalization of fullerenes[44] and SWCNTs,[45,46] while SWCNHs have been also recently functionalized in this way with the aid of microwaves.[47] Herein, we demonstrate a powerful way to exfoliate graphite through a simple sonication step creating stable suspensions and then proceed to covalently attach organic moieties onto the graphene skeleton, using the Bingel reaction and applying microwave irradiation conditions. Stable dispersions of cyclopropanated graphene are obtained, while the electroactive moiety of extended tetrathiafulvalene (exTTF) is incorporated. The graphene-based nanohybrids are characterized by complementary spectroscopic (Raman, ATR-IR), thermal gravimetric analysis (TGA) and high-resolution electron microscopy (HR-TEM) techniques. Finally, the electrochemical redox potentials of graphene−exTTF nanohybrid are evaluated by cyclic voltametry (CV), while the presence of sulfur in the graphene−exTTF nanohybrid was verified by electron dispersive X-ray (EDX).

RESULTS AND DISCUSSION

Inspired by Coleman's approach to use an appropriate solvent capable of overcoming the van der Waals interactions of graphite we opted to try out the possibility of benzylamine in order to produce graphene sheets from exfoliation of graphite. The electron donating character of benzylamine may play a role on the exfoliation of few-graphene layers most likely by forming charge-transfer complexes with them. At first, benzylamine was added to graphite flakes and the mixture was sonicated for a moderate time of 2−6 h. Even from the early stages of sonication a gray and then an ink-like solution was forming. By the end of the sonication treatment, the afforded dispersion could be easily separated from the unaffected graphite through centrifugation and remained stable for a few days.

At this stage it is important to point to a very recent and thorough study presenting exfoliation of graphite using *N*-methyl-pyrrolidone (NMP).[43] In short, that study involves the effect of various aspects, such as sonication time, energy output of the sonication bath as well as the work up centrifugation, on the exfoliation outcome. In our case, the relatively short sonication time applied is indicative of our intention not only to provide an alternative efficient solvent for exfoliation of graphite, but more importantly to use the resulting material as a basis for covalent functionalization of graphene. Therefore, several aspects of this study, such as severe defect formation, owed to sonication, or solvent degradation due to excessive heating of the bath, can be overlooked.

To explore the efficiency of the selected benzylamine solvent, DMF was also tried for longer periods of time with no appreciable results. Also *o*-dichlorobenzene (oDCB) was recently reported[48] to be a fair solvent for the exfoliation of graphite, but in our case it was not as efficient. With the use of 2 mL of benzylamine and 7 mg of graphite and sonication for 2−4 h, a stable solution with a concentration of ∼0.5 mg/mL can be obtained. This was measured by drying and weighing the graphite precipitate after centrifugation and removal of the supernatant suspension. Longer sonication periods (∼10 h) did not seem to increase the reported concentration of graphene in benzylamine. When high centrifugation speed (4000 rpm) was applied, the concentration of 0.5 mg/mL of graphene in benzylamine was evaluated.

Sonication in a solvent creates defects onto graphene sheets,[43] however these are situated mostly on the edges, rather than on the graphene surface, leaving mostly intact the electronic properties of the material. In our case, compared to pristine graphite flakes, careful examination of the Raman spectra revealed an increase of the I_D/I_G ratio (Figure 1) denoting that defects are introduced through the sonication procedure with benzylamine. This is most likely attributed to generation of new edges created by the exfoliation of graphite.

Raman spectroscopy is a powerful tool for studying graphene as it can reveal the extent of exfoliation,[34,43,49,50] which at the same time can follow changes caused by hole and electron doping.[51−53] Therefore, it is not surprising that the 2D band at 2700 cm^{-1} has also changed shape from a sharp band to a more featureless broader peak indicative of the number of layers per flake. Although in our study, single graphene sheets possessing sharp and symmetric 2D

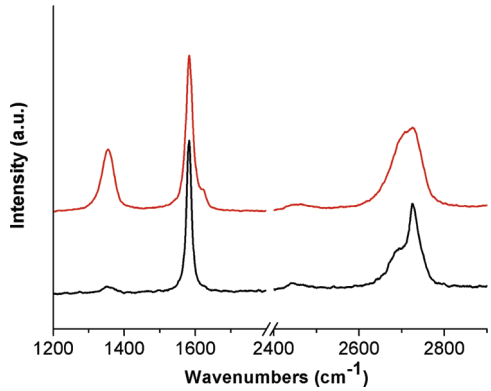

Figure 1. Raman spectra, using 514 nm excitation line, of graphite (black) and exfoliated graphene after typical sonication with benzylamine (red).

band cannot be identified, the Raman spectrum of the benzylamine treated graphite is indicative of graphene particles consisting of few graphene sheets. More drastic changes in the Raman spectrum are observed upon functionalization, as reported below.

The solubility achieved through the use of benzylamine allowed us to proceed to the next level, namely functionalize graphene with organic groups. Tour and co-workers recently proposed initial exfoliation with oDCB to allow for radical addition of alkyl iodides onto graphenes.[48] Moreover, during the course of the current study, exfoliation of graphene with the aid of pyridine or NMP, followed by implementation of 1,3-dipolar cycloaddition reaction of azomethine ylides affording pyrrolidine decorated graphene sheets was reported.[54,55] Encouraged by our previous attempt to functionalize SWCNHs under microwave irradiation using the Bingel reaction conditions,[47] we opted to covalently attach malonate-bearing organic moieties onto the graphitic skeleton of the nanomaterial.

Microwave-assisted chemistry is an important tool in carbon nanostructure chemistry. During the past decade several publications exhibiting advantages of microwave-assisted chemistry *versus* conventional synthetic approaches dealing with fullerenes,[56] carbon nanotubes[57−60] and carbon nanohorns[61] have surfaced. Microwave chemistry takes advantage of the strong microwave absorption that carbon nanostructures exhibit toward mw irradiation,[62,63] facilitating reactions carried out under it. Moreover, it affords flexibility, reduced amount of time required for said reaction and in most cases reported, cleaner products. 1,8-Diazabicyclo[5.4.0]undec-7-ene (DBU) and CBr_4[64,65] were used alongside the diethylmalonate, to functionalize graphene (Scheme 1).

In Table 1 the reaction conditions are presented for each of the attempted functionalization reactions. At this point it is worth noting that attempted exfoliation with an inappropriate solvent (*i.e.*, toluene) and application of the same experimental conditions (reagents/microwave intensity/exposure) did not yield any soluble product. Moreover, in another blank experiment, simply mixing graphite flakes and reagents for the cyclopropanation reaction, under microwave irradiation, did not furnish products. Therefore, Bingel reaction conditions are not applicable when pre-exfoliation of the graphene does not take place, at least under microwaves. As such, the type of solvent, is crucial to the functionalized material produced and should be taken into account.

In the absence of air cooling during the reaction, (Table 1, entry 1) the amount of microwave irradiation is smaller due to rapid increase in temperature. In all other samples, air cooling was used, which allowed for higher intensity of irradiation to be applied for prolonged periods of time, combined with the stepwise reaction sequence for better temperature control. A typical plot of the power/time evolution throughout the various steps of the reaction is presented at the Supporting Information (Figure S1).

Besides the diethyl malonate readily available, the electroactive extended tetrathiafulvalene (exTTF) derivative (**2**) was chosen, in order to investigate the electrochemistry of the nanomaterial. The exTTF (**2**) was synthesized according to literature procedures,[66] and was covalently added onto the graphene network with the aid of microwave irradiation.

During early attempts to exfoliate and functionalize graphene, larger quantities of solvent (benzylamine) were used, up to 8 mL for 10 mg of graphite. However, low yields of Bingel functionalized graphene were obtained (<0.5 mg), indicating that concentration plays an important role in the reaction conditions. We, thus, opted to use a smaller solvent volume in order to keep concentration high. Using an excess of commercially available diethylmalonate, this holds true. Therefore,

TABLE 1. Experimental Details for the Microwave Assisted Functionalization of Graphene

entry	material	graphite (mg)	malonate (mmol)	CBr_4 (mg)	benzylamine (mL)	step 1 (watt/sec)	step 2 (watt/sec)	step 3 (watt/sec)
1	**G1**	12	2.6	690	1.5	5/300		
2	**G1**[a]	10	4.2	700	1.5	10/200	30/180	
3	**G1**[a]	1[c]	2.6	650	2	30/180	30/180	30/180
4	**G2**[a]	7	0.19[b]	670	1.5	30/180	10/180	10/180
5	**G2**[a]	1[c]	0.05[b]	630	2	20/180	20/180	20/180

[a]Denotes that active cooling was used during microwave reaction. [b]Denotes that the exTTF malonate derivative was used. [c]Denotes that the exfoliation mixture was centrifuged and only the supernatant was used for the reaction.

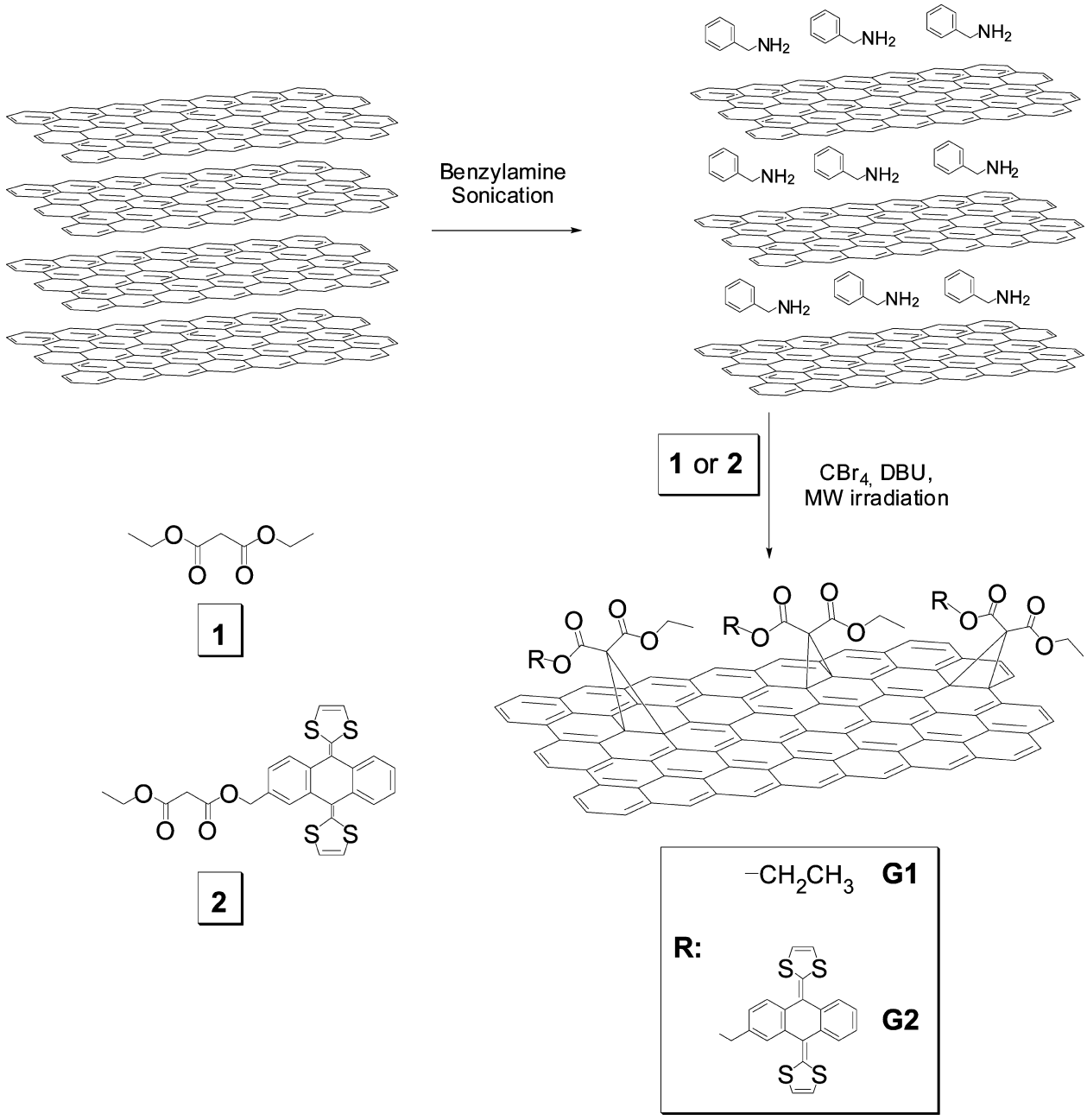

Scheme 1. Synthetic procedure affording functionalized graphene-based materials G1 and G2.

the volume of benzylamine was kept to a maximum of 2 mL in all experiments.

Following the reaction on the microwave oven, the yielded nanohybrid material was filtrated and washed several times with DMF, methanol, and dichloromethane (DCM) to remove excess organic content not attached to the graphene skeleton. Then the residue was suspended in DCM and centrifuged. The supernatant formed stable dispersions for several days in various organic solvents (DCM, *o*-DCB, DMF, toluene), enhancing the notion that functionalization indeed took place. The enhanced solubility achieved for the Bingel-functionalized graphenes allowed us to perform studies in solution. Thus, the electronic absorption spectrum UV−vis−NIR of **G1** material in DCM was recorded, showing a continuous absorbance from the UV to the NIR region. Similarly, the UV−vis−NIR spectrum of **G2** was also featureless with a continuous absorbance throughout the recorded spectral regions with the exTTF absorbance being masked and flattened (Supporting Information, Figure S2).

Pristine graphite shows an almost featureless infrared spectrum. In contrast, in the attenuated-total-reflectance infrared (ATR-IR) spectra of **G1** and **G2**, the presence of the characteristic C−H stretching vibrations due to the grafted malonate moieties at 2920 and 2847 cm^{-1} is evident (Supporting Information, Figure S3); as well the carbonyl vibration due to malonate units are

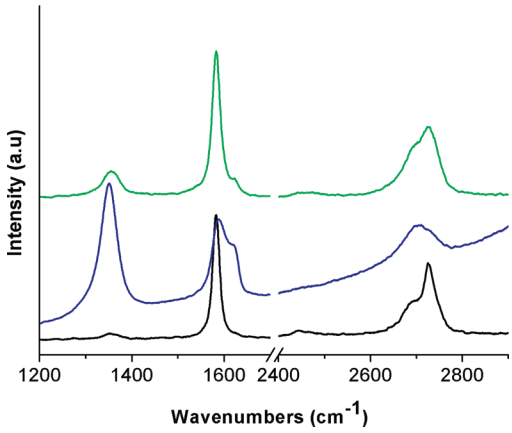

Figure 2. Raman spectra, using 514 nm excitation line of graphite (black), functionalized graphene hybrid material G2 (blue), and residual material after thermogravimetric analysis measurements (green).

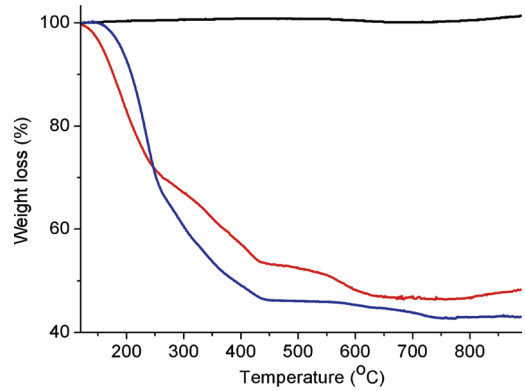

Figure 3. Thermogravimetric analysis of intact graphite (black) and functionalized graphene materials G1 (blue) and G2 (red).

also seen at around 1705 and 1727 cm^{-1}, respectively, providing significant support for the successful covalent functionalization. Moreover, the stretching bands due to the carbon−carbon double bonds are observed at around 1600 cm^{-1}, similarly with intact graphite.

In Figure 2, the Raman spectra of the cyclopropanated graphene material, graphite, and exfoliated graphene are compared. When Bingel reaction conditions are applied, the I_D/I_G ratio is completely changed and the D-band intensity is increased surpassing the G-band, thus supporting covalent grafting of malonate moieties onto the graphene layers. Moreover, the 2D band changes dramatically, indicating the smaller number of graphene sheets existing in a given flake.[49] We also examined the material after thermal decomposition of the organic units attached. In this context, when thermogravimetric analysis (TGA) measurements were conducted on the **G2** material, under an inert atmosphere, the Raman spectrum returns to a form resembling the initial graphite one, showing substantial changes in the D, G, and 2D bands as compared with the corresponding ones in the Raman spectrum of the functionalized material (Figure 2). The process of heating up the sample to 900 °C increases, as expected, the number of defect sites on the graphitic skeleton, as exhibited by a greater I_D/I_G ratio when compared with the ratio of those present in intact graphite. Examination of both functionalized graphene hybrid materials, **G1** and **G2**, reveals the same trend with an elevated I_D/I_G ratio compared to that of the pristine graphite.

TGA measurements were also used to determine the organic content of the samples. We noticed that benzylamine with a boiling point of around 180 °C is a difficult solvent to remove from the samples. However, as pointed out earlier, the functionalization procedure, allowed for efficient dispersion in a number of volatile solvents such as DCM. Subsequently, continuous washing and centrifugation of the samples using volatile solvents would decrease the chance that residual benzylamine will affect our TGA measurements considerably.

In Figure 3 the TGA graphs of both **G1** and **G2** materials are presented and compared with that of intact graphite. The latter is thermally stable when heated up to 900 °C under nitrogen; however, functionalized materials **G1** and **G2** show considerable weight loss due to the decomposition of the covalently grafted organic addends. As benzylamine, having a high boiling point of 185 °C, was initially used to achieve exfoliation of few-graphene sheets, prior to the microwave-assisted Bingel functionalization, it is reasonable to assume that the weight loss observed in **G1** and **G2** up to 240 °C corresponds to entrapped benzylamine within graphene layers. Therefore, the weight loss observed in the temperature range 240−450 °C is attributed to the thermal decomposition of the malonate units and is calculated to be 23% and 18% for materials **G1** and **G2**, respectively. On the basis of those values, the number of graphene carbon atoms per malonate moiety is estimated, thus giving a functionalization degree of 1 diethyl malonate unit per 44 carbon atoms and 1 exTTF malonate unit per 198 carbon atoms, in **G1** and **G2** materials, respectively. The difference in functionalization can be rationalized by the steric hindrances introduced by the bulkier exTTF moiety (compared to diethylmalonate) influencing the organic uptake of the final product. The weight loss observed above 600 °C is attributed to the thermal decomposition of defects created at sites where functionalization occurred, consistent with the behavior exhibited by similarly functionalized carbon nanostructures, like carbon nanotubes and carbon nanohorns.[60,67,68]

When one tries to morphologically examine samples to determine more accurately the efficient exfoliation of graphene, atomic force microscopy (AFM) is widely used. However in the case of benzylamine-sonicated exfoliated graphenes, the high boiling point of the solvent would cause severe aggregation,[43] thus prohibiting proper morphological examination. However, HR-TEM examination was performed to morphologically

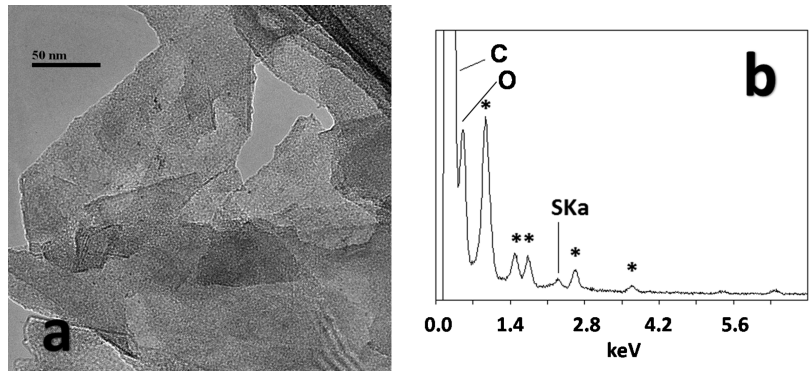

Figure 4. (a) Representative HR-TEM image and (b) EDX spectra of functionalized graphene hybrid material G2. Asterisks denote impurities due to the elements of Cu, Fe, Al, and Si which are present in the microscope equipment, sample holder and crystal detector.

evaluate the condition of the exfoliated modified graphene hybrid material. In Figure 4a, a typical HR-TEM image of material **G2** is shown. It is clear that few-layer graphene sheets are present; however, the exact number of graphene layers cannot be estimated and no large graphitic aggregates are found denoting that efficient exfoliation indeed took place. Moreover in the specific sample, EDX measurements (Figure 4b) were carried out to confirm the presence of sulfur atoms, strengthening the notion that covalent functionalization took place anchoring exTTF moieties along the graphitic skeleton. Additionally, a representative HR-TEM image and the corresponding EDX spectrum of material **G1** are shown at the Supporting Information (Figure S4).

The electrochemical properties of graphene−exTTF **G2** were also studied by cyclic voltammetry (CV). The CV measurements were performed in CH_2Cl_2 containing 0.1 M *n*-Bu_4NPF_6 as a supporting electrolyte, with Pt disk (1.6 mm diameter) as working electrode and Pt gauze, with a 52 mesh, as counter-electrode. The measured potentials were recorded with the aid of a silver wire immersed in $AgNO_3$, 0.1 M in dry CH_3CN as reference. In Figure 5 the cyclic voltammogram of the **G2** is depicted. Two peaks are clearly discernible: a weak oxidation peak at 0.35 V *vs* Fc/Fc^+ that is attributed to the exTTF moiety, corresponding to the formation of the dication species,[69−71] shifted by 55 mV with respect to

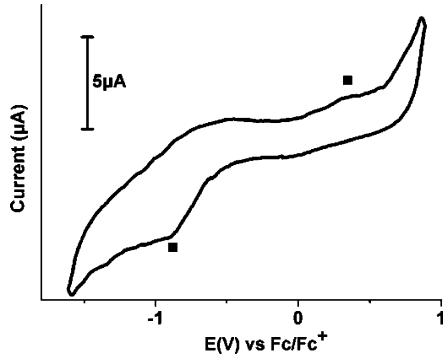

Figure 5. Cyclic voltammogram of G2 obtained in 0.1 M $TBAPF_6$ in CH_2Cl_2 using $Ag/AgNO_3$ as reference electrode. Scan rate is 100 mV/s.

the pristine exTTF moiety, and a broad reduction peak at −0.88 V *vs* Fc/Fc^+ attributed to the reduction of functionalized graphene (see also Supporting Information, Figure S5, the CV of material **G1**). This result suggests the possibility of the formation of a radical ion pair that includes one-electron oxidation of exTTF, namely $(exTTF)^{\bullet+}$ and one-electron reduction of graphene, namely $(graphene)^{\bullet-}$. The energy gap, which is the total energy for the radical ion pair, of $(graphene)^{\bullet-}-(exTTF)^{\bullet+}$, calculated as the difference between the oxidation potential of exTTF and the reduction potential of graphene, was found to be 1.23 eV. Therefore, the free-energy change for the charge-separated state of $(graphene)^{\bullet-}-(exTTF)^{\bullet+}$, *via* the formation of the singlet excited state of exTTF, namely $^1(exTTF)^*$ with a total energy of 1.91 eV,[72] was evaluated to be −0.69 eV, which confirms the exothermic formation process of $(graphene)^{\bullet-}-(exTTF)^{\bullet+}$.

CONCLUSIONS

A novel and efficient solvent capable of creating stable graphene suspensions from graphite was introduced in the form of benzylamine, and its efficiency during simple sonication of intact graphite was established. This allowed the use of the exfoliated graphene dispersion to covalently graft malonate moieties along the graphitic skeleton, following the Bingel reaction conditions and using microwave irradiation. The reaction conditions provided highly functionalized products, improving solubility in various organic solvents. The graphene-based hybrid materials were characterized by using complementary spectroscopic, thermal, and microscopy techniques. Electro-active moieties, in the form of malonate bearing extended tetrathiafulvalene units, were covalently attached onto the graphene skeleton and the presence of sulfur in the hybrid material was confirmed by EDX spectroscopy. Electrochemical examination of the exTTF−graphene hybrid material allowed the determination of the redox potentials, while the formation of a radical ion pair that includes one-electron oxidation of exTTF and one-electron reduction of graphene was suggested.

EXPERIMENTAL SECTION

Chemicals. All reagents were purchased from Aldrich and were used without further purification, unless otherwise stated. The malonate modified π-extended tetrathiafulvalene (exTTF)[73−75] was synthesized according to literature methods.[66]

Instrumentation. For the microwave synthesis, a CEM Discover microwave reactor with infrared pyrometer and pressure control system was used. For sonication a SOLTEC, Sonica 3300ETH ultrasonic cleaner was used. Midinfrared spectra in the region 550−4000 cm^{-1} were obtained on a Fourier transform IR spectrometer (Equinox 55 from Bruker Optics) equipped with a single reflection diamond ATR accessory (DuraSamp1IR II by SensIR Technologies). Raman measurements were performed at room temperature with a Renishaw confocal spectrometer at 514 nm. The thermogravimetric analysis was performed using a TGA Q500 V20.2 Build 27 instrument by TA in an inert atmosphere of nitrogen. In a typical experiment 1 mg of the material was placed in the sample pan and the temperature was equilibrated at 100 °C. Subsequently, the temperature was increased to 900 °C with a rate of 10 °C/min and the weight changes were recorded as a function of temperature. Electrochemistry studies were performed using a standard three-electrode cell with Pt disk (1.6 mm diameter) as a working electrode, Pt mesh as counter-electrode and $Ag/AgNO_3$ (0.1 M $AgNO_3$ in acetonitrile) as a reference electrode. Cyclic voltammograms were carried out in dried CH_2Cl_2 using $TBAPF_6$ (recrystallized three times from acetone and dried in a vacuum at 100 °C before each experiment) as electrolyte, under N_2 atmosphere. Ferrocene was used as an internal standard. Measurements were recorded using an EG&G Princeton Applied Research potensiostat/galvanostat model 2273 connected to a personal computer running PowerSuite software. HR-TEM measurements and EDX analysis were performed using a JEOL JEM 2100F microscope equipped with a superatmospheric thin-window X-ray detector.

Exfoliation of Graphite. The appropriate amount of graphite flakes and benzylamine were added in a glass vessel under argon atmosphere; the vessel was sealed and sonicated for $t \approx 2-10$ h. The resulting black ink-like dispersion was centrifuged to remove the larger graphite aggregates. The solubility of graphene in benzylamine is estimated at around 0.5 mg/mL.

General Method for Microwave-Assisted Bingel Functionalization of Exfoliated Graphene. To the suspended solution of graphene in benzylamine, 1,8-diazabicyclo[5.4.0]undec-7-ene (DBU), carbon tetrabromide (CBr_4), and the corresponding malonate derivative were added. The mixture was purged with Ar, sealed, and left to react in the microwave oven for the appropriate time using 130 °C as a temperature threshold. Upon completion, *N,N*-dimethylformamide (DMF) was added to the reaction mixture, and following filtration under vacuum the solid was washed with DMF, methanol, and CH_2Cl_2. The black powder was sonicated and centrifuged repeatedly until a colorless supernatant was obtained. The combined supernatants were filtered affording the product.

Acknowledgment. This work was partially supported by the EU FP7, Capacities Program, NANOHOST project (GA 201729) and COST network MP0901 NanoTP.

Supporting Information Available: Microwave power-temperature *vs* time plots, UV−vis and ATR-IR spectra, HR-TEM images, EDX data, and cyclic voltammograms for materials discussed in the manuscript. This material is available free of charge *via* the Internet at http://pubs.acs.org.

REFERENCES AND NOTES

1. Novoselov, K. S.; Geim, A. K.; Morozov, S. V.; Jiang, D.; Zhang, Y.; Dubonos, S. V.; Grigorieva, I. V.; Firsov, A. A. Electric Field Effect in Atomically Thin Carbon Films. *Science* **2004**, *306*, 666–669.
2. Iijima, S. Helical Microtubules of Graphitic Carbon. *Nature* **1991**, *354*, 56–58.
3. Hirsch, A. The Chemistry of the Fullerenes: An Overview. *Angew. Chem., Int. Ed.* **1993**, *32*, 1138–1141.
4. Iijima, S.; Yudasaka, M.; Yamada, R.; Bandow, S.; Suenaga, K.; Kokai, F.; Takahashi, K. Nano-aggregates of Single-Walled Graphitic Carbon Nanohorns. *Chem. Phys. Lett.* **1999**, *309*, 165–170.
5. Novoselov, K. Graphene: Mind the Gap. *Nat. Mater.* **2007**, *6*, 720–721.
6. Westervelt, R. M. Applied Physics: Graphene Nanoelectronics. *Science* **2008**, *320*, 324–325.
7. Sutter, P. Epitaxial Graphene: How Silicon Leaves the Scene. *Nat. Mater.* **2009**, *8*, 171–172.
8. Novoselov, K. S.; Geim, A. K.; Morozov, S. V.; Jiang, D.; Katsnelson, M. I.; Grigorieva, I. V.; Dubonos, S. V.; Firsov, A. A. Two-Dimensional Gas of Massless Dirac Fermions in Graphene. *Nature* **2005**, *438*, 197–200.
9. Zhang, Y.; Tan, Y.-W.; Stormer, H. L.; Kim, P. Experimental Observation of the Quantum Hall Effect and Berry's Phase in Graphene. *Nature* **2005**, *438*, 201–204.
10. Meyer, J. C.; Geim, A. K.; Katsnelson, M. I.; Novoselov, K. S.; Booth, T. J.; Roth, S. The Structure of Suspended Graphene Sheets. *Nature* **2007**, *446*, 60–63.
11. Heersche, H. B.; Jarillo-Herrero, P.; Oostinga, J. B.; Vandersypen, L. M. K.; Morpurgo, A. F. Bipolar Supercurrent in Graphene. *Nature* **2007**, *446*, 56–59.
12. Ohta, T.; Bostwick, A.; Seyller, T.; Horn, K.; Rotenberg, E. Controlling the Electronic Structure of Bilayer Graphene. *Science* **2006**, *313*, 951–954.
13. Novoselov, K. S.; Jiang, Z.; Zhang, Y.; Morozov, S. V.; Stormer, H. L.; Zeitler, U.; Maan, J. C.; Boebinger, G. S.; Kim, P.; Geim, A. K. Room-Temperature Quantum Hall Effect in Graphene. *Science* **2007**, *315*, 1379.
14. Tombros, N.; Jozsa, C.; Popinciuc, M.; Jonkman, H. T.; van Wees, B. J. Electronic Spin Transport and Spin Precession in Single Graphene Layers at Room Temperature. *Nature* **2007**, *448*, 571–574.
15. Wang, Y.; Huang, Y.; Song, Y.; Zhang, X.; Ma, Y.; Liang, J.; Chen, Y. Room-Temperature Ferromagnetism of Graphene. *Nano Lett.* **2008**, *9*, 220–224.
16. Stankovich, S.; Dikin, D. A.; Dommett, G. H. B.; Kohlhaas, K. M.; Zimney, E. J.; Stach, E. A.; Piner, R. D.; Nguyen, S. T.; Ruoff, R. S. Graphene-Based Composite Materials. *Nature* **2006**, *442*, 282–286.
17. Dikin, D. A.; Stankovich, S.; Zimney, E. J.; Piner, R. D.; Dommett, G. H. B.; Evmenenko, G.; Nguyen, S. T.; Ruoff, R. S. Preparation and Characterization of Graphene Oxide Paper. *Nature* **2007**, *448*, 457–460.
18. Li, D.; Kaner, R. B. Materials Science: Graphene-Based Materials. *Science* **2008**, *320*, 1170–1171.
19. Lee, C.; Wei, X.; Kysar, J. W.; Hone, J. Measurement of the Elastic Properties and Intrinsic Strength of Monolayer Graphene. *Science* **2008**, *321*, 385–388.
20. Bunch, J. S.; van der Zande, A. M.; Verbridge, S. S.; Frank, I. W.; Tanenbaum, D. M.; Parpia, J. M.; Craighead, H. G.; McEuen, P. L. Electromechanical Resonators from Graphene Sheets. *Science* **2007**, *315*, 490–493.
21. Balandin, A. A.; Ghosh, S.; Bao, W.; Calizo, I.; Teweldebrhan, D.; Miao, F.; Lau, C. N. Superior Thermal Conductivity of Single-Layer Graphene. *Nano Lett.* **2008**, *8*, 902–907.
22. Baughman, R. H.; Zakhidov, A. A.; de Heer, W. A. Carbon Nanotubes: The Route Toward Applications. *Science* **2002**, *297*, 787–792.
23. Li, X.; Zhang, G.; Bai, X.; Sun, X.; Wang, X.; Wang, E.; Dai, H. Highly Conducting Graphene Sheets and Langmuir−Blodgett Films. *Nat. Nanotechnol.* **2008**, *3*, 538–542.
24. Xu, Y.; Liu, Z.; Zhang, X.; Wang, Y.; Tian, J.; Huang, Y.; Ma, Y.; Zhang, X.; Chen, Y. A Graphene Hybrid Material Covalently Functionalized with Porphyrin: Synthesis and Optical Limiting Property. *Adv. Mater.* **2009**, *21*, 1275–1279.
25. Kim, K. S.; Zhao, Y.; Jang, H.; Lee, S. Y.; Kim, J. M.; Kim, K. S.; Ahn, J.-H.; Kim, P.; Choi, J.-Y.; Hong, B. H. Large-Scale Pattern Growth of Graphene Films for Stretchable Transparent Electrodes. *Nature* **2009**, *457*, 706–710.
26. Pan, Y.; Zhang, H.; Shi, D.; Sun, J.; Du, S.; Liu, F.; Gao, H.-J. Highly Ordered, Millimeter-Scale, Continuous, Single-Crystalline Graphene Monolayer Formed on Ru (0001). *Adv. Mater.* **2009**, *21*, 2777–2780.

27. Sutter, P. W.; Flege, J.-I.; Sutter, E. A. Epitaxial Graphene on Ruthenium. *Nat. Mater.* **2008**, *7*, 406–411.
28. Kosynkin, D. V.; Higginbotham, A. L.; Sinitskii, A.; Lomeda, J. R.; Dimiev, A.; Price, B. K.; Tour, J. M. Longitudinal Unzipping of Carbon Nanotubes to Form Graphene Nanoribbons. *Nature* **2009**, *458*, 872–876.
29. Jiao, L.; Zhang, L.; Wang, X.; Diankov, G.; Dai, H. Narrow Graphene Nanoribbons from Carbon Nanotubes. *Nature* **2009**, *458*, 877–880.
30. Xuekun, L.; Yu, M.; Huang, H.; Ruoff, R. S. Tailoring Graphite with the Goal of Achieving Single Sheets. *Nanotechnology* **1999**, *10*, 269.
31. Novoselov, K. S.; Jiang, D.; Schedin, F.; Booth, T. J.; Khotkevich, V. V.; Morozov, S. V.; Geim, A. K. Two-Dimensional Atomic Crystals. *Proc. Natl. Acad. Sci. U.S.A.* **2005**, *102*, 10451–10453.
32. Su, Q.; Pang, S.; Alijani, V.; Li, C.; Feng, X.; Müllen, K. Composites of Graphene with Large Aromatic Molecules. *Adv. Mater.* **2009**, *21*, 3191–3195.
33. Wang, H.; Robinson, J. T.; Li, X.; Dai, H. Solvothermal Reduction of Chemically Exfoliated Graphene Sheets. *J. Am. Chem. Soc.* **2009**, *131*, 9910–9911.
34. Hernandez, Y.; Nicolosi, V.; Lotya, M.; Blighe, F. M.; Sun, Z.; De, S.; McGovern, I. T.; Holland, B.; Byrne, M.; Gun'Ko, Y. K.; *et al.* High-Yield Production of Graphene by Liquid-Phase Exfoliation of Graphite. *Nat. Nanotechnol.* **2008**, *3*, 563–569.
35. Lotya, M.; Hernandez, Y.; King, P. J.; Smith, R. J.; Nicolosi, V.; Karlsson, L. S.; Blighe, F. M.; De, S.; Wang, Z.; McGovern, I. T.; *et al.* Liquid Phase Production of Graphene by Exfoliation of Graphite in Surfactant/Water Solutions. *J. Am. Chem. Soc.* **2009**, *131*, 3611–3620.
36. Si, Y.; Samulski, E. T. Synthesis of Water Soluble Graphene. *Nano Lett.* **2008**, *8*, 1679–1692.
37. Jung, I.; Pelton, M.; Piner, R.; Dikin, D. A.; Stankovich, S.; Watcharotone, S.; Hausner, M.; Ruoff, R. S. Simple Approach for High-Contrast Optical Imaging and Characterization of Graphene-Based Sheets. *Nano Lett.* **2007**, *7*, 3569–3575.
38. Stankovich, S.; Dikin, D. A.; Piner, R. D.; Kohlhaas, K. A.; Kleinhammes, A.; Jia, Y.; Wu, Y.; Nguyen, S. T.; Ruoff, R. S. Synthesis of Graphene-Based Nanosheets *via* Chemical Reduction of Exfoliated Graphite Oxide. *Carbon* **2007**, *45*, 1558–1565.
39. Wang, X.; Zhi, L.; Mullen, K. Transparent, Conductive Graphene Electrodes for Dye-Sensitized Solar Cells. *Nano Lett.* **2007**, *8*, 323–327.
40. Li, D.; Muller, M. B.; Gilje, S.; Kaner, R. B.; Wallace, G. G. Processable Aqueous Dispersions of Graphene Nanosheets. *Nat. Nanotechnol.* **2008**, *3*, 101–105.
41. Allen, M. J.; Tung, V. C.; Gomez, L.; Xu, Z.; Chen, L.-M.; Nelson, K. S.; Zhou, C.; Kaner, R. B.; Yang, Y. Soft Transfer Printing of Chemically Converted Graphene. *Adv. Mater.* **2009**, *21*, 2098–2102.
42. Fowler, J. D.; Allen, M. J.; Tung, V. C.; Yang, Y.; Kaner, R. B.; Weiller, B. H. Practical Chemical Sensors from Chemically Derived Graphene. *ACS Nano* **2009**, *3*, 301–306.
43. Khan, U.; O'Neill, A.; Lotya, M.; De, S.; Coleman, J. N. High-Concentration Solvent Exfoliation of Graphene. *Small* **2010**, *6*, 864–871.
44. Diederich, F.; Thilgen, C. Covalent Fullerene Chemistry. *Science* **1996**, *271*, 317–324.
45. Coleman, K. S.; Bailey, S. R.; Fogden, S.; Green, M. L. H. Functionalization of Single-Walled Carbon Nanotubes *via* the Bingel Reaction. *J. Am. Chem. Soc.* **2003**, *125*, 8722–8723.
46. Tasis, D.; Tagmatarchis, N.; Bianco, A.; Prato, M. Chemistry of Carbon Nanotubes. *Chem. Rev.* **2006**, *106*, 1105–1136.
47. Economopoulos, S. P.; Pagona, G.; Yudasaka, M.; Iijima, S.; Tagmatarchis, N. Solvent-Free Microwave-Assisted Bingel Reaction in Carbon Nanohorns. *J. Mater. Chem.* **2009**, *19*, 7326–7331.
48. Hamilton, C. E.; Lomeda, J. R.; Sun, Z.; Tour, J. M.; Barron, A. R. High-Yield Organic Dispersions of Unfunctionalized Graphene. *Nano Lett.* **2009**, *9*, 3460–3462.
49. Ferrari, A. C.; Meyer, J. C.; Scardaci, V.; Casiraghi, C.; Lazzeri, M.; Mauri, F.; Piscanec, S.; Jiang, D.; Novoselov, K. S.; Roth, S.; *et al.* Raman Spectrum of Graphene and Graphene Layers. *Phys. Rev. Lett.* **2006**, *97*, 187401.
50. Malard, L. M.; Pimenta, M. A.; Dresselhaus, G.; Dresselhaus, M. S. Raman Spectroscopy in Graphene. *Phys. Rep.* **2009**, *473*, 51–87.
51. Das, A.; Pisana, S.; Chakraborty, B.; Piscanec, S.; Saha, S. K.; Waghmare, U. V.; Novoselov, K. S.; Krishnamurthy, H. R.; Geim, A. K.; Ferrari, A. C.; *et al.* Monitoring Dopants by Raman Scattering in an Electrochemically Top-Gated Graphene Transistor. *Nat. Nanotechnol.* **2008**, *3*, 210–215.
52. Rakesh, V.; Das, B.; Rout, C. S.; Rao, C. N. R. Effects of Charge Transfer Interaction of Graphene with Electron Donor and Acceptor Molecules Examined Using Raman Spectroscopy and Cognate Techniques. *J. Phys.: Condens. Matter* **2008**, *20*, 472204.
53. Das, B.; Voggu, R.; Rout, C. S.; Rao, C. N. R. Changes in the Electronic Structure and Properties of Graphene Induced by Molecular Charge-Transfer. *Chem. Commun.* **2008**, 5155–5157.
54. Georgakilas, V.; Bourlinos, A.; Zboril, R.; Steriotis, T.; Dallas, P.; Stubos, A.; Trapalis, C. Organic Functionalisation of Graphenes. *Chem. Commun.* **2010**, *46*, 1766–1769.
55. Quintana, M.; Spyrou, K.; Grzelczak, M.; Browne, W. R.; Rudolf, P.; Prato, M. Functionalization of Graphene *via* 1,3-Dipolar Cycloaddition. *ACS Nano* **2010**, *4*, 3527–3533.
56. de la Cruz, P.; de la Hoz, A.; Langa, F.; Illescas, B.; Martin, N. Cycloadditions to [60]Fullerene Using Microwave Irradiation: A Convenient and Expeditious Procedure. *Tetrahedron* **1997**, *53*, 2599–2608.
57. Delgado, J. L.; Cruz, P. d. l.; Langa, F.; Urbina, A.; Casado, J.; Navarrete, J. T. L. Microwave-Assisted Sidewall Functionalization of Single-Wall Carbon Nanotubes by Diels−Alder Cycloaddition. *Chem. Commun.* **2004**, 1734–1735.
58. Umeyama, T.; Tezuka, N.; Fujita, M.; Matano, Y.; Takeda, N.; Murakoshi, K.; Yoshida, K.; Isoda, S.; Imahori, H. Retention of Intrinsic Electronic Properties of Soluble Single-Walled Carbon Nanotubes after a Significant Degree of Sidewall Functionalization by the Bingel Reaction. *J. Phys. Chem. C* **2007**, *111*, 9734–9741.
59. Brunetti, F. G.; Herrero, M. A.; Munoz, J. d. M.; Giordani, S.; Diaz-Ortiz, A.; Filippone, S.; Ruaro, G.; Meneghetti, M.; Prato, M.; Vazquez, E. Reversible Microwave-Assisted Cycloaddition of Aziridines to Carbon Nanotubes. *J. Am. Chem. Soc.* **2007**, *129*, 14580–14581.
60. Brunetti, F. G.; Herrero, M. A.; Munñoz, J. d. M.; Diáz-Ortiz, A.; Alfonsi, J.; Meneghetti, M.; Prato, M.; Vaźquez, E. Microwave-Induced Multiple Functionalization of Carbon Nanotubes. *J. Am. Chem. Soc.* **2008**, *130*, 8094–8100.
61. Rubio, N.; Herrero, M. A.; Meneghetti, M.; Diaz-Ortiz, A.; Schiavon, M.; Prato, M.; Vazquez, E. Efficient Functionalization of Carbon Nanohorns *via* Microwave Irradiation. *J. Mater. Chem.* **2009**, *19*, 4407–4413.
62. Imholt, T. J.; Dyke, C. A.; Hasslacher, B.; Perez, J. M.; Price, D. W.; Roberts, J. A.; Scott, J. B.; Wadhawan, A.; Ye, Z.; Tour, J. M. Nanotubes in Microwave Fields: Light Emission, Intense Heat, Outgassing, and Reconstruction. *Chem. Mater.* **2003**, *15*, 3969–3970.
63. Vaźquez, E.; Prato, M. Carbon Nanotubes and Microwaves: Interactions, Responses, and Applications. *ACS Nano* **2009**, *3*, 3819–3824.
64. Nierengarten, J.-F.; Gramlich, V.; Cardullo, F.; Diederich, F. Regio- and Diastereoselective Bisfunctionalization of C_{60} and Enantioselective Synthesis of a C_{60} Derivative With a Chiral Addition Pattern. *Angew. Chem., Int. Ed. Engl.* **1996**, *35*, 2101–2103.
65. Nakamura, Y.; Minami, S.; Iizuka, K.; Nishimura, J. Preparation of Neutral [60] Fullerene-Based [2]Catenanes and [2]Rotaxanes Bearing an Electron-Deficient Aromatic Diimide Moiety. *Angew. Chem., Int. Ed.* **2003**, *42*, 3158–3162.

66. Gonzalez, S.; Martin, N.; Guldi, D. M. Synthesis and Properties of Bingel-type Methanofullerene-π-Extended-TTF Diads and Triads. *J. Org. Chem.* **2003**, *69*, 779–791.
67. Titus, E.; Ali, N.; Cabral, G.; Gracio, J.; Ramesh Babu, P.; Jackson, M. Chemically Functionalized Carbon Nanotubes and Their Characterization Using Thermogravimetric Analysis, Fourier Transform Infrared, and Raman Spectroscopy. *J. Mater. Eng. Perform.* **2006**, *15*, 182–186.
68. Pagona, G.; Karousis, N.; Tagmatarchis, N. Aryl Diazonium Functionalization of Carbon Nanohorns. *Carbon* **2008**, *46*, 604–610.
69. Guldi, D. M.; Sánchez, L.; Martín, N. Formation and Characterization of the π-Radical Cation and Dication of π-Extended Tetrathiafulvalene Materials. *J. Phys. Chem. B* **2001**, *105*, 7139–7144.
70. Herranz, M.Á.; Martin, N.; Campidelli, S.; Prato, M.; Brehm, G.; Guldi, D. M. Control Over Electron Transfer in Tetrathiafulvalene-Modified Single-Walled Carbon Nanotubes. *Angew. Chem., Int. Ed.* **2006**, *45*, 4478–4482.
71. Gayathri, S.; Wielopolski, M.; Pérez, E.; Fernández, G.; Sánchez, L.; Viruela, R.; Ortí, E.; Guldi, D.; Martín, N. Discrete Supramolecular Donor-Acceptor Complexes. *Angew. Chem., Int. Ed.* **2009**, *48*, 815–819.
72. Herranz, M. A.; Martín, N.; Sánchez, L.; Seoane, C.; Guldi, D. M. New [pi]-Extended Tetrathiafulvalene-Containing Fulleropyrrolidine Dyads Endowed With Vinyl Spacers. *J. Organomet. Chem.* **2000**, *599*, 2–7.
73. Martin, N.; Perez, I.; Sanchez, L.; Seoane, C. Synthesis and Properties of the First Highly Conjugated Tetrathiafulvalene Analogues Covalently Attached to [60]Fullerene. *J. Org. Chem.* **1997**, *62*, 5690–5695.
74. Herranz, M. A.; Martín, N. A New Building Block for Diels–Alder Reactions in π-Extended Tetrathiafulvalenes: Synthesis of a Novel Electroactive C_{60}-Based Dyad. *Org. Lett.* **1999**, *1*, 2005–2007.
75. Martin, N.; Sanchez, L.; Guldi, D. Stabilisation of Charge-Separated States *via* Gain of Aromaticity and Planarity of the Donor Moiety in C_{60}-Based Dyads. *Chem. Commun.* **2000**, 113–114.